Response Time Improvement of Liquid Crystal Reflectarray Using Partition Wall Structure

Yuhao Shang, Graduate Student Member, IEEE, Hiroyasu Sato, Member, IEEE, Kai-Da Xu, Senior Member, IEEE, Masakazu Nakatani, Member, IEEE, Yasuo Yamamoto, Hideo Fujikake, Senior Member, IEEE, and Qiang Chen, Senior Member, IEEE

Abstract—In this letter, we propose a new structure for liquid crystal reflectarray (LCRA) aimed at improving response time. In LCRA, liquid crystal (LC) serves as a phase-tunable material that can be continuously modulated by an external electric field. However, the inherently slow response time of LC remains a significant limitation for practical applications. To address this issue, we introduce a structure incorporating partition walls with vertical alignment films on the surface of the LCRA. This design induces an additional anchoring force on the LC layer, facilitating faster reorientation of LC molecules, which results in significant reduce of the response time. For validation, an LCRA prototype based on the proposed structure was fabricated and experimentally measured. The results demonstrate a substantial improvement in response performance, with the decay time reduced from 6.62 s to 0.73 s. It is believed that the proposed LCRA structure will be a promising candidate for future RA applications.

Index Terms—Liquid crystal (LC), millimeter wave, reflectarray (RA), response time.

I. INTRODUCTION

POR the next generation of wireless communications, base station antennas are required to support high gain, high frequency, and rapid beam scanning capabilities. Reconfigurable intelligent surfaces (RISs) have emerged as a promising technology to meet these demands, with reflectarray (RA) being a representative implementation [1]. RA can achieve beam control by adjusting the phase and amplitude of individual elements, thereby enhancing the electromagnetic (EM) signal in a targeted region or enabling dynamic beam steering. This functionality allows RA to effectively address the coverage needs of complex environments [2], [3].

Different control methods for RAs have been explored, including those based on diodes [4]–[6], mechanical actuation [7]–[9], and liquid crystal (LC) technology [10]–[17]. Mechanical control approach is structurally complicated, which also suffers from slow response time, while MEMS and diodebased methods often involve high cost and face challenges in assembly and integration. In contrast, LC offers several

This work was supported by the Ministry of Internal Affairs and Communications in Japan (JPJ000254).

Yuhao Shang, Hiroyasu Sato, and Qiang Chen are with the Department of Communications Engineering, Tohoku University, Sendai 980-8579, Japan.

Kai-Da Xu is with the Department of Signal Theory and Communications, Polytechnic School, University of Alcalá, 28871 Alcalá de Henares, Spain (e-mail: kaidaxu@ieee.org).

Masakazu Nakatani, Yasuo Yamamoto and Hideo Fujikake is with the Department of Electronic Engineering, Tohoku University, Sendai 980-8579, Japan.

advantages, such as low cost and ease of compatibility with planar structures, making it suitable for RA applications. Moreover, LC molecules can be reoriented by an external electric field, enabling continuous tuning of permittivity. With this property, liquid crystal reflectarrays (LCRAs) can achieve more precise beam scanning.

Despite the many advantages of liquid crystals (LCs), their inherently slow response time remains a major challenge. The response time consists of the rise and decay times. The rise time mainly depends on the applied voltage and can be shortened by increasing the bias voltage, whereas reducing the decay time is more difficult, attracting significant research attention [18], [19]. One approach to shorten the decay time is introducing a polymer network into the LC layer [18]. The polymer network anchors the LC molecules and strengthens intermolecular forces, thereby accelerating relaxation. However, it reduces the dielectric anisotropy and reflection phase range. The increased intermolecular force also demands a higher bias voltage for reorientation. Another method employs dual-frequency LC (DFLC) [19], which exhibits both positive and negative dielectric anisotropy frequencies [20]. Under a positive frequency bias, LC molecules align parallel to the electric field, whereas under a negative frequency, they orient perpendicularly. DFLCs offer faster decay than nematic LCs but suffer from high loss tangent and require a complex bias network.

In this letter, an LCRA employing a partition-wall structure coated with vertical alignment films is proposed. This structure introduces additional anchoring forces to accelerate the recovery of LC molecules without excessively restricting their reorientation under bias voltage, thereby effectively shortening the decay time while maintaining a sufficient reflection phase variation range. The remaining parts of this letter are organized as follows. Section II introduces the detailed configuration of the partition wall structure, with simulation results for validating its effectiveness. In Section III, the measured performance of fabricated LCRA prototypes with and without partition walls is demonstrated, which validates that the proposed structure significantly reduces decay time. Finally, Section IV concludes this work.

II. STRUCTURE AND ANALYSIS

In previous studies of LCRAs, a conventional structure comprising a superstrate, electrodes, and a metal ground plane combined with planar alignment films has been widely adopted to control the orientation of LC molecules [21]–[23]. When a bias voltage is applied, the LC molecules are reoriented in response to the electric field across the LC layer. When the bias voltage is removed, the molecules gradually return to their initial state due to the surface anchoring effect imposed by the planar alignment layers on both the upper and lower interfaces of the LC layer [24]. For such a configuration, the decay time τ_d can be given as [25], [26]:

$$\tau_d = \frac{\gamma h_{LC}^2}{K\pi^2} \tag{1}$$

where γ is the rotational viscosity, K is the elastic constant of the LC, and h_{LC} is the thickness of the LC layer. Observed from the condition $\tau_d \propto h_{LC}^2$, the decay time is greatly affected by the thickness of the LC layer. Increasing the LC layer thickness typically results in a longer decay time. On the other hand, reducing the LC thickness will unfortunately lead to the increase of reflection loss [27]. This trade-off highlights a key limitation of the conventional configuration: when a thicker LC layer is employed, the LC molecules near the center of the layer will be farther from the alignment film surface, where the anchoring effect will be weaker. As a result, the molecules in the central region respond more slowly than those near the alignment films, leading to an extended decay time for the LCRA.

To reduce the decay time, a partition wall structure coated with polyimide vertical alignment films is embedded into the LC layer. The LC is sandwiched between a superstrate and a metal ground plane, both of which are coated with polyimide planar alignment films. The partition walls are coated with vertical alignment films on their surfaces [28]. The LC layer is divided by partition walls, with each LC segment occupying a volume equal to the gap between adjacent walls. Both the planar and vertical alignment films exert anchoring forces that promote horizontal orientation of the LC molecules. The configurations of the LC cell using partition wall structure without and with bias voltages are illustrated in Fig. 1(a) and Fig. 1(b), respectively. After removal of the bias voltage, this enhanced anchoring effect facilitates a faster relaxation of the LC molecules back to their initial state, thereby reducing the overall response time.

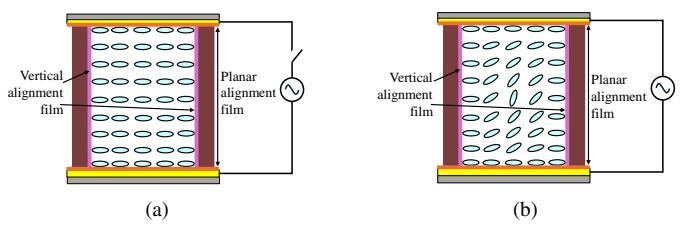


Fig. 1. LC molecules states inside the partition wall structure (a) without bias voltage, and (b) with bias voltage.

The proposed unit cell structure of LCRA is depicted in Fig. 2(a) and a zoom-in view of proposed partition wall structure is depicted in Fig. 2(b). It consists of five parts arranged from top to bottom: the superstrate, multi-resonant structure, LC, partition walls and metal ground, where the partition

walls are placed inside the LC layer as depicted in Fig. 2(c). The multi-resonant structure is constructed by a dual size-different patch connected with bias line, as depicted in Fig. 2(d), which can provide sufficient reflection phase variation, and the patch dimensions are optimized to maximize the achievable reflection phase variation. Planar alignment films are deposited on the superstrate and the metal ground to control the orientation of LC molecules toward x-direction, and the vertical alignment films were deposited on the surface of partition walls further force LC molecules oriented toward x-direction, which is helpful to improve the response time of LCRA.

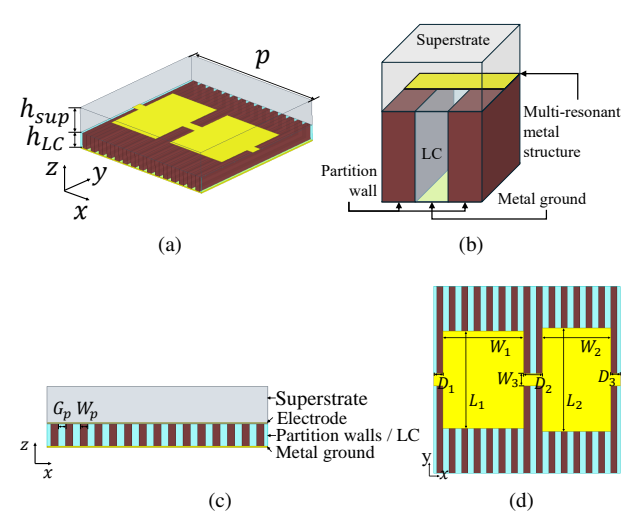


Fig. 2. (a) Perspective view, (b) zoom-in view (c) side view and (d) top view of the proposed LCRA unit cell structure. The parameters are $W_p = G_p = 0.02$ mm, $L_1 = 1.56$ mm, $L_2 = 1.66$ mm, $W_1 = 1.30$ mm, $W_2 = 1.10$ mm, $W_3 = 0.20$ mm, $D_1 = D_3 = 0.15$ mm, $D_2 = 0.30$ mm, $D_3 =$

A simulation was conducted using LCD Master software [29] to evaluate the decay time of the proposed LC structure with different partition wall spacings. The structure for simulation is depicted in Fig. 3(a). The anchoring energy of alignment films is set as 10^{-5} J/m² matching the polyimide alignment films used in this letter. The partition wall spacing G_p is set from 20 µm to 50 µm, while maintaining a constant LC layer thickness of 45 µm. ZOC LC was used in all cases, and a bias voltage of 40 V was applied. In the simulation, the decay time is defined as the duration required for the normalized capacitance of proposed LC structure to decrease from 100 % to 10 %, representing the relaxation process of LC molecules following the removal of the bias voltage. The decay time for different wall spacings G_p is presented in Fig. 3(b). Since the partition walls are coated with vertical alignment films, reducing the spacing between adjacent walls decreases the distance between these films. Consequently, the alignment films exert a stronger influence on the LC molecules in the central region of the LC layer, which facilitates faster molecular reorientation and thereby shortens the LC decay time. Among the simulated configurations, the structure with 20 µm spacing exhibits the shortest decay time. Considering the fabrication limitation, partition wall spacing and width are limited to 20 µm for simulation and measurement in subsequent experiments.

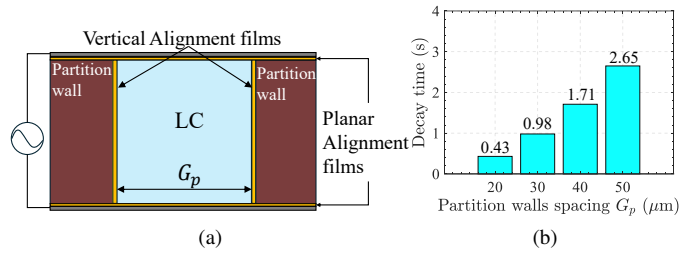


Fig. 3. (a) Structure for simulation (b) Simulated decay time with different spacings of partition walls.

Consequently, the proposed LCRA structure is analyzed using full-wave electromagnetic simulation where the partition wall is made by SU-8 3000 permanent photoresist $(\varepsilon_r = 3.72, \tan \delta = 0.03)$. The superstrate material is nonalkali glass ($\varepsilon_{rG}=5.4, \tan\delta=0.007$). The corresponding reflection magnitude and phase are presented in Fig. 4(a) and Fig. 4(b), respectively. The LC used for simulation is ZOC whose relative permittivity and loss tangent under full bias voltage and zero bias voltage are $\varepsilon_{r\perp}=2.56$, $\tan\delta_{\perp}=0.006$, $\varepsilon_{r/\!\!/}=3.80,\, \tan\delta_{/\!\!/}=0.003.$ It can be observed that as the bias voltage increases (i.e., $\varepsilon_{r\perp} \to \varepsilon_{r/\!\!/}$), the resonant frequencies of the proposed LCRA are shifted to lower frequencies, thereby altering the reflection magnitude and phase at certain frequency points. The maximum amount of reflection phase variation is 481°, observed at 45.2 GHz. The phase variation range of larger than 360° is seen to be sufficient for the RA design to ensure the large angle beam steering ability of the proposed LCRA.

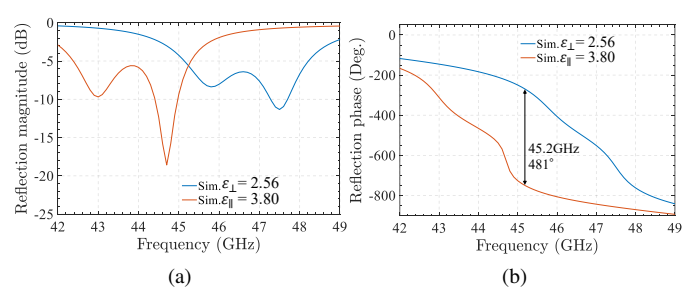


Fig. 4. Simulated frequency responses of (a) reflection magnitude and (b) reflection phase of the proposed LCRA unit cell.

The top and side views of the LCRA unit without partition walls (i.e., the conventional LCRA structure) employing single-patch and two-patch structures are presented in Fig. 5(a) and Fig. 5(b), respectively. The simulated reflection phases corresponding to these structures are presented in Fig. 5(c). Compared with the conventional LCRA structure, the proposed LCRA exhibits a relatively smaller reflection phase variation since the partition walls partially occupy the LC layer region. The two-patch structure is adopted to compensate for this reduction, which significantly broadens the reflection phase variation compared with that of the single-patch structure. Consequently, the proposed LCRA still achieves a reflection phase variation exceeding 360°.

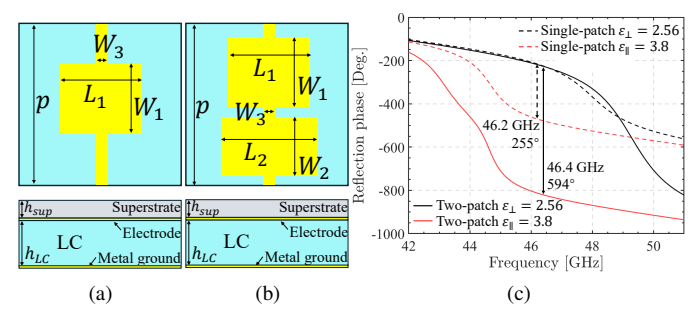


Fig. 5. Top and side views of the LCRA unit without partition walls employing (a) single-patch and (b) two-patch structures. (c) Simulated frequency responses of the reflection phases for the single-patch and two-patch structures filled with ZOC LC.

III. MEASUREMENT RESULTS

The proposed LCRA was fabricated for experimental verification. The partition walls were constructed using SU-8 3000 permanent photoresis fabricated by Dai Nippon Printing (DNP) Co., Ltd. Fig. 6(a) presents two fabricated LCRA samples, each of which is a 15×17 unit array, with and without the partition wall structure encapsulated within the LC layer. The partition walls have a spacing and width of 20 μm , and a height of 45 μm , thereby maintaining a uniform LC layer thickness of 45 μm . For a fair comparison, 45 μm -thick spacers were used in the LCRA without partition walls to ensure the same LC layer thickness in both devices.

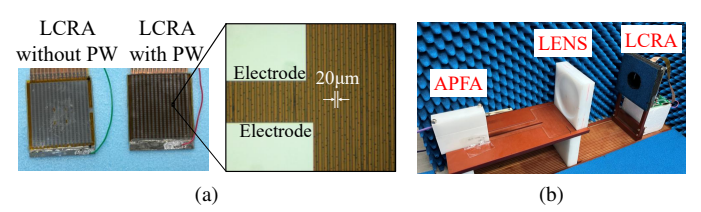


Fig. 6. (a) The prototypes of the proposed LCRA (PW = partition wall), (b) the measurement environment with APFA and lens.

The reflection phase of LCRAs is measured by lens-load printed antipodal fermi tapered slot antenna (APFA) [30], using the Keysight Network Analyzer P5008A, as shown in Fig. 6(b). The low-frequency bias voltages are generated by a computer-controlled NF Multifunction Generator WF1974 and amplified by NF High-Speed Power Amplifier 4005.

The measured frequency responses of the proposed LCRA are presented in Fig. 7. A maximum reflection phase variation of 447° is achieved at 45.3 GHz, which deviates from the simulated result. This deviation is not attributed to insufficient bias voltage, as the reflection phase remains nearly constant with negligible variation when the applied voltage approaches 40 V. Instead, the deviation arises from the vertical alignment films coated on the surfaces of the partition walls. These films impose anchoring forces that hinder the reorientation of LC molecules near the wall surfaces under bias voltage, thereby restricting the overall deflection of the LC molecules and reducing the achievable phase variation of the proposed LCRA.

Fig. 8(a) presents the measured decay times of the LCRAs with and without partition walls. The measurements were performed after applying a stabilized bias voltage of 40 V, which was removed 1 s after the start of measurement. For the LCRA with partition walls, the response time was measured at 45.3 GHz, where the maximum reflection phase variation of 447° was obtained. For the LCRA without partition walls, the maximum reflection phase variation of 589° was observed at 46.3 GHz, and the response time was measured at 44.75 GHz, where the same reflection phase variation as that of the partition-wall-based LCRA was achieved. The difference in operating frequency between the two structures arises because the embedded partition walls alter the effective permittivity of the LC layer. Nevertheless, the proposed partition wall structure imposes no inherent frequency limitation, since its effect is limited to the LC layer. In this study, the decay time of the LCRA is defined as the duration required for the reflection phase to reach 90% of its maximum variation after the bias voltage is removed. The LCRA without partition walls exhibits a decay time of 6.62 s, whereas the LCRA with partition walls achieves a markedly shorter decay time of 0.73 s. These results clearly demonstrate that the proposed partition wall structure can significantly reduce the decay time of the LCRA.

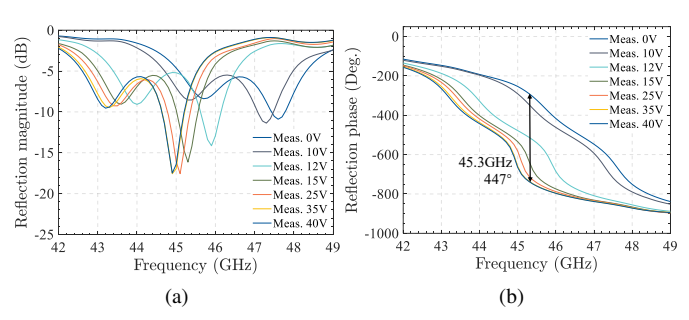


Fig. 7. Measured frequency responses of (a) reflection magnitude and (b) reflection phase of the proposed LCRA under different bias voltages.

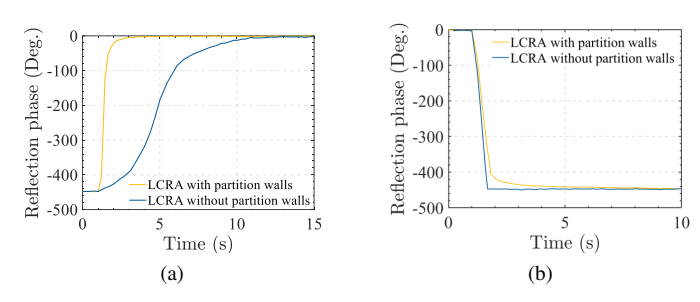


Fig. 8. Measured response time of (a) rise time and (b) decay time of the proposed LCRA unit cell.

Fig. 8(b) shows the measured rise times of the two LCRA structures. The rise time is defined as the duration required for the reflection phase to reach 90% of its maximum variation after the application of the bias voltage. A 40 V bias voltage was applied 1 s after the measurement began. The LCRA with partition walls exhibits a rise time of 0.81 s, whereas the LCRA without partition walls shows a shorter rise time of 0.61 s. As expected, the presence of partition

TABLE I COMPARISONS WITH PRIOR WORKS

	[15]	[16]	[18]	[19]	This work
Frequency (GHz)	37.5	100	100	100	45.3
Technology	Conventional LC	LC + OD	LC + PN	DF LC	PWS
LC thickness (mm)	0.2	0.075	0.045	0.045	0.045
Phase range (deg.)	338	360	180	360	447
Rise time (s)	1.05	0.05	0.012	5	0.81
Decay time (s)	6.05	5	0.21	2	0.73

LC+OD = liquid crystal + overdrive; LC+PN = liquid crystal + polymer network; DFLC = dual-frequency liquid crystal; PWS = partition wall structure.

walls slightly increases the rise time due to the additional horizontal anchoring force. However, this increase is relatively minor compared with the significant improvement in decay time. Therefore, the measurement results confirm that partition walls with vertical alignment films substantially improve the overall response performance of the LCRA. Table I provides a comparison between the proposed LCRA and several previous works. As can be seen, the proposed structure achieves a significantly shorter decay time while maintaining a sufficient reflection phase variation range.

IV. CONLUSION

In this work, a partition wall structure was embedded into the LC layer to improve response time of the LCRA. Vertical alignment films were applied to the surfaces of the partition walls to provide additional anchoring effects, thereby shortening the decay time. Two 15 \times 17 unit LCRAs were fabricated and measured, one with partition walls and the other without partition walls for performance comparison. Measurement results show that the proposed LCRA with partition walls achieves a reflection phase variation of 447° at 45.3 GHz, enabling wide-angle beam scanning capability. More significantly, the response time is reduced from 7.23 s to 1.54 s. The proposed LCRA sacrifices only a portion of the reflection phase variation range in exchange for a significant reduction in response time. Although the proposed structure is more complicated to fabricate compared with the conventional ones, the inclusion of partition walls enables approximately a 50% reduction in LC consumption. The proposed LCRA maintains a sufficient reflection phase variation range while significantly reducing the response time, making it a promising candidate for future high-speed and wide-angle beam scanning LCRA applications.

ACKNOWLEDGMENT

The authors would like to express their sincere appreciation to Mr. Yoshi Naonobu and Mr. Hayakawa Mamoru from DNP for their partial contributions to this work.

REFERENCES

- E. Basar, M. Di Renzo, J. De Rosny, M. Debbah, M.-S. Alouini, and R. Zhang, "Wireless communications through reconfigurable intelligent surfaces," *IEEE Access*, vol. 7, pp. 116753–116773, 2019.
- [2] D. Pozar, S. Targonski, and R. Pokuls, "A shaped-beam microstrip patch reflectarray," *IEEE Trans. Antennas Propag*, vol. 47, no. 7, pp. 1167– 1173, 1999.
- [3] A. Yu, F. Yang, A. Z. Elsherbeni, J. Huang, and Y. Kim, "An offset-fed x-band reflectarray antenna using a modified element rotation technique," *IEEE Trans. Antennas Propag*, vol. 60, no. 3, pp. 1619–1624, 2012.
- [4] W. Wu, K.-D. Xu, Q. Chen, T. Tanaka, M. Kozai, and H. Minami, "A wideband reflectarray based on single-layer magneto-electric dipole elements with 1-bit switching mode," *IEEE Trans. Antennas Propag*, vol. 70, no. 12, pp. 12346–12351, 2022.
- [5] M. Wang, S. Xu, F. Yang, and M. Li, "A 1-bit bidirectional reconfigurable transmit-reflect-array using a single-layer slot element with pin diodes," *IEEE Trans. Antennas Propag*, vol. 67, no. 9, pp. 6205–6210, 2019
- [6] X. Cao, Q. Chen, T. Tanaka, M. Kozai, and H. Minami, "A 1-bit time-modulated reflectarray for reconfigurable-intelligent-surface applications," *IEEE Trans. Antennas Propag*, vol. 71, no. 3, pp. 2396–2408, 2023
- [7] W. Menzel, D. Pilz, and M. Al-Tikriti, "Millimeter-wave folded reflector antennas with high gain, low loss, and low profile," *IEEE Antennas Propag Mag*, vol. 44, no. 3, pp. 24–29, 2002.
- [8] X. Yang, S. Xu, F. Yang, M. Li, H. Fang, Y. Hou, S. Jiang, and L. Liu, "A mechanically reconfigurable reflectarray with slotted patches of tunable height," *IEEE AWP Letters*, vol. 17, no. 4, pp. 555–558, 2018.
- [9] A. Hu, K. Konno, Q. Chen, and T. Takahashi, "A highly efficient 1-bit reflectarray antenna using electromagnet-controlled elements," *IEEE Trans. Antennas Propag*, vol. 72, no. 1, pp. 506–517, 2024.
- [10] S. Bildik, S. Dieter, C. Fritzsch, W. Menzel, and R. Jakoby, "Reconfigurable folded reflectarray antenna based upon liquid crystal technology," *IEEE Trans. Antennas Propag*, vol. 63, no. 1, pp. 122–132, 2015.
- [11] X. Li, Y. Wan, J. Liu, D. Jiang, T. Bai, K. Zhu, J. Zhuang, and W.-Q. Wang, "Broadband electronically scanned reflectarray antenna with liquid crystals," *IEEE AWP Letters*, vol. 20, no. 3, pp. 396–400, 2021.
- [12] Y. Cui, H. Sato, K.-D. Xu, H. Fujikake, and Q. Chen, "A method of dual-bias voltage supply for reducing reflection loss in reconfigurable intelligent surfaces of liquid crystal," *IEEE AWP Letters*, vol. 23, no. 11, pp. 3529–3533, 2024.
- [13] M. Y. Ismail, R. Cahill, M. Amin, A. F. M. Zain, and M. K. Amin, "Phase range analysis of patch antenna reflectarray based on nematic liquid crystal substrate with dynamic rcs variation," in 2007 Asia-Pacific Microwave Conference, 2007, pp. 1–4.
- [14] W. Hu, R. Cahill, J. A. Encinar, R. Dickie, H. Gamble, V. Fusco, and N. Grant, "Design and measurement of reconfigurable millimeter wave reflectarray cells with nematic liquid crystal," *IEEE Trans. Antennas Propag*, vol. 56, no. 10, pp. 3112–3117, 2008.
- [15] X. Li, H. Sato, H. Fujikake, and Q. Chen, "Development of two-dimensional steerable reflectarray with liquid crystal for reconfigurable intelligent surface applications," *IEEE Trans. Antennas Propag*, vol. 72, no. 3, pp. 2108–2123, 2024.
- [16] R. Guirado, G. Perez-Palomino, M. Ferreras, E. Carrasco, and M. Caño-García, "Dynamic modeling of liquid crystal-based metasurfaces and its application to reducing reconfigurability times," *IEEE Trans. Antennas Propag*, vol. 70, no. 12, pp. 11847–11857, 2022.
- [17] T. Haneda, T. Ishinabe, Y. Shibata, H. Sato, Q. Chen, and H. Fujikake, "Fabrication of lc-polymer films separating thick lc layer for reflect arrays," *ITE Transactions on Media Technology and Applications*, vol. 10, no. 4, pp. 146–151, 2022.
- [18] R. Guirado, G. Perez-Palomino, M. Caño-García, M. A. Geday, and E. Carrasco, "mm-wave metasurface unit cells achieving millisecond response through polymer network liquid crystals," *IEEE Access*, vol. 10, pp. 127 928–127 938, 2022.
- [19] R. Guirado, P. de la Rosa, G. Perez-Palomino, M. Caño-García, E. Carrasco, and X. Quintana, "Characterization and application of dual-frequency liquid-crystal mixtures in mm-wave reflectarray cells to improve their temporal response," *IEEE Trans. Antennas Propag*, vol. 71, no. 8, pp. 6535–6545, 2023.
- [20] X. Liang, Y.-Q. Lu, Y.-H. Wu, F. Du, H.-Y. Wang, and S.-T. Wu, "Dual-frequency addressed variable optical attenuator with submillisecond response time," *Japanese journal of applied physics*, vol. 44, no. 3R, p. 1292, 2005.

- [21] S. Bildik, C. Fritzsch, A. Moessinger, and R. Jakoby, "Tunable liquid crystal reflectarray with rectangular elements," in *German Microwave Conference Digest of Papers*, 2010, pp. 1–4.
- [22] L. Cai, Z. H. Jiang, and W. Hong, "Evaluation of reconfigurable reflectarray antenna element at 19 ghz based on highly anisotropic liquid crystal material," in 2019 IEEE International Conference on Computational Electromagnetics (ICCEM), 2019, pp. 1–3.
- [23] G. Perez-Palomino, J. A. Encinar, M. Barba, R. Dickie, P. Baine, R. Cahill, R. Florencio, and R. R. Boix, "Wideband unit-cell based on liquid crystals for reconfigurable reflectarray antennas in f-band," in Proceedings of the 2012 IEEE International Symposium on Antennas and Propagation, 2012, pp. 1–2.
- [24] O. Melnyk, Y. Garbovskiy, D. Bueno-Baques, and A. Glushchenko, "Electro-optical switching of dual-frequency nematic liquid crystals: Regimes of thin and thick cells," *Crystals*, vol. 9, no. 6, 2019. [Online]. Available: https://www.mdpi.com/2073-4352/9/6/314
- [25] X. Nie, H. Xianyu, R. Lu, T. X. Wu, and S.-T. Wu, "Pretilt angle effects on liquid crystal response time," *Journal of Display Technology*, vol. 3, no. 3, pp. 280–283, 2007.
- [26] P. G. de Gennes and J. Prost, The Physics of Liquid Crystals, 2nd ed. Oxford University Press, 1993.
- [27] Y. Cui, H. Sato, Y. Shibata, T. Ishinabe, H. Fujikake, and Q. Chen, "A low-cost structure for reducing reflection loss in intelligent reflecting surface of liquid crystal," *IEEE AWP Letters*, vol. 22, no. 12, pp. 3027– 3031, 2023.
- [28] T. Haneda, T. Ishinabe, Y. Shibata, H. Sato, Q. Chen, and H. Fujikake, "Thick lc devices stabilized by polymer wall surface for millimeter wave control," *Proceedings of the International Display Workshops*, vol. 29, p. 97 – 100, 2022.
- [29] Shintech Optics Co., Ltd., "LCD Master Software," http://www.shintechopt.com/lcd-master, 2024.
- [30] H. SATO, Y. TAKAGI, and K. SAWAYA, "High gain antipodal fermi antenna with low cross polarization," *IEICE Trans. Commun*, vol. E94.B, no. 8, pp. 2292–2297, 2011.